Behavior of quartz forks oscillating in isotopically pure ^{4}He in the $T \rightarrow 0$ limit

Deepak Garg,[1] V. B. Efimov,[1,2] M. Giltrow,[1] P. V. E. McClintock,[1] L. Skrbek,[3] and W. F. Vinen[4]

[1]*Department of Physics, Lancaster University, Lancaster LA1 4YB, United Kingdom*
[2]*Institute of Solid State Physics RAS, Chernogolovka, Moscow region, 142432 Russia*
[3]*Faculty of Mathematics and Physics, Charles University, Ke Karlovu 3, 121 16 Prague, Czech Republic*
[4]*School of Physics and Astronomy, University of Birmingham, B15 2TT, United Kingdom*

We report that at low drives, the resonant frequencies and linewidths of nominally 32-kHz quartz tuning forks oscillating in isotopically pure superfluid ^{4}He at $\sim$10 mK are dependent on the dimensions of their environment. We confirm the importance of coupling between forks and acoustic modes within the cell, and develop a theory of their coupled dynamics to account for the observations. The frequencies and linewidths are reproducible on a time scale of tens of minutes, but pronounced drifts are seen over longer intervals. We suggest that the drifts are attributable to changes in the velocity of sound due to tiny pressure changes. In studies at high drives, we observe two critical velocities: $v_{c1} \approx 0.6$ cm/s, where the drag may either increase or decrease, depending on the linewidth; and $v_{c2} \approx 10$ cm/s, above which there seems to be fully turbulent flow. At high drives, the behavior of the drag differs markedly between forks that appear otherwise to be very similar.

I. INTRODUCTION

In recent years, small quartz tuning forks, such as are used as frequency standards in watches, have been used extensively in measurements at low temperatures. They are small and easy to operate and install. Applications have ranged from their use as thermometers, pressure sensors, and viscometers in all the helium fluids[1] to the study of the generation of both classical[2–4] and quantum turbulence[1,4–11] in both ^{3}He and ^{4}He by an oscillating structure. By the term quantum turbulence (QT) we mean turbulence in a superfluid, where it can be strongly influenced by two-fluid effects and by the quantization of circulation.

The original aim of the work reported here was a study of the damping of the oscillations of a fork associated with the transition at high drives from laminar flow to quantum turbulence in isotopically pure ^{4}He in the low-temperature limit. In this limit, there is no normal fluid, and the turbulence is influenced only by the quantization of circulation, which requires that rotational motion can be generated solely through the presence of quantized vortex lines. Our experimental set up is described in Sec. II. At low drives, there should be potential flow of the helium (all superfluid) past the prongs of a vibrating fork, so that the damping should not be in excess of that observed *in vacuo* at the same temperature. However, it soon became clear that in fact the low-drive damping is larger, often much larger, and that both the damping and the resonant frequency drift in time (Sec. III). In parallel with our own work, other authors observed and reported similar effects,[12,13] which they attributed to acoustic emission by the vibrating fork. Tentatively, they suggested that the acoustic emission could lead to a coupling between the oscillations of a fork and the standing acoustic modes in the surrounding helium. The fact that these acoustic modes depend on the design and dimensions of the cell in which a fork oscillates means that the environment of a fork can strongly influence its behavior. In Sec. V A, we argue in general terms that acoustic coupling is indeed important. In Sec. V B, we report calculations from which we estimate the strength of the coupling to the acoustic modes in our apparatus, and we demonstrate that our observations of the damping of our fork at low drives can indeed be accounted for in terms of acoustic coupling, the time dependence of the damping, and the resonant frequency arising from slow and very small drifts in the velocity of sound in the helium associated with very small drifts in the pressure. Having understood, we believe, these acoustic effects, we returned to studies of the transition to turbulence, our experimental results being described in Sec. IV. A discussion of these results is presented in Secs. V C and V D. Our conclusions are summarized in Sec. VI.

It may be helpful to comment on some general aspects of this paper. Our discussion of acoustic coupling effects occupies a substantial fraction of the paper. Matters relating to quantum turbulence occupy a smaller fraction. More importantly, the experimental results relating to QT are in a sense disappointing. They show that the drag on the prongs of a fork due to the generation of QT varies from fork to fork, even when the forks are apparently identical. This confusing lack of reproducibility must mean that small differences between forks, such as might be associated with surface roughness, are important, and it is possible that this sensitivity to small differences is characteristic of quantum turbulence at very low temperatures. Any systematic study of this sensitivity would be difficult and time consuming, and, in the absence of any technique for visualizing the turbulent flow, would very probably be uninformative.

II. EXPERIMENTAL SETUP

The experiments were performed in a ^{3}He-^{4}He dilution refrigerator at its base temperature of $\sim$10 mK. The large experimental cell, holding $\sim$1.5 ℓ of isotopically pure ^{4}He under pressures of up to 5 bar, has been described elsewhere.[14–16] We investigate nominally 32-kHz quartz tuning forks[17] mounted in a number of different environments. The basic parameters of the forks used are given in Table I.

In the first set of experiments, three forks f1, f2, f3, were mounted in "free space" within the cell. Two of these (f1 and

TABLE I. Dimensions of the forks used in the experiments, and their resonance parameters at ∼10 mK *in vacuo*. L is the length of a prong, the cross section of which is $W \times T$, where T is the dimension parallel to direction of movement of the prong (Ref. [18]). The separation between the inner surfaces of the two prongs is close to 0.2 mm in all cases. The fork constant a is the ratio between the displacement current and the velocity of the prong and acts as the bridge between the fork's electrical and mechanical properties.

Fork	L (mm)	W (mm)	T (mm)	f (Hz)	Δf (Hz)	$10^5 a$ (C/m)
f1	3.68	0.26	0.6	32708.23	0.068	1.05
f2	3.12	0.35	0.4	32711.05	0.134	0.89
f3	3.68	0.26	0.6	32704.36	0.080	1.07
F1	3.75	0.26	0.6	32710.98	0.028	1.05
F2	3.75	0.26	0.6	32723.25	0.024	1.06
F3	3.75	0.26	0.6	32712.36	0.016	1.09
F4	3.75	0.26	0.6	32709.36	4.000	

f2) are shown in Fig. 1(a); the third one (f3, not shown) was mounted outside the main electrode structure.

The second set of experiments involved four forks F1, F2, F3, F4 from a different batch by the same manufacturer. They were individually housed in four open-ended cylindrical tubes made out of paper impregnated with Stycast 1266, as shown in Fig. 1(b). F1 remained within its original vacuum can, but with a 0.4-mm hole drilled in the top of the can. F2–F4 were bare, as were f1–f3 in the first set of experiments. It had been intended that the dimensions of the tubes containing F1, F2, and F4 would be such that no acoustic mode would be in resonance with a fork, but in fact the diameters turned out to be such that one of the radial mode resonances was close to 32 kHz; as we shall see, this may be a significant factor in relation to some aspects of the observed behavior.

The cell was filled very slowly (over about 100 h) with isotopically pure superfluid ^{4}He (^{3}He fraction less[19] than 10^{-12}) while keeping its temperature well below 1 K. In some cases, the cell was initially cooled to $T \sim 10$ mK under vacuum. After measurements had been made of the forks' vacuum responses, it was filled with superfluid ^{4}He as before. The current response of each fork was monitored with a custom-made I-V converter,[20] the output of which was measured using a Stanford SR830 lock-in amplifier. LABVIEW programs were used (a) to sweep the frequency of the drive through resonance at a fixed drive amplitude or (b) to lock the drive frequency to the top of the resonance while, e.g., the drive amplitude was being changed. It was assumed that, for a fixed drive amplitude, the linewidth was inversely proportional to the maximum value of the response.

III. EXPERIMENTS ON THE RESPONSE TO A LOW DRIVE

A. Oscillations in vacuum

To obtain reliable vacuum measurements at low temperatures, the cell was flushed repeatedly with dry nitrogen gas prior to cooling so that no helium film could form on the forks at low temperatures. The low-drive linewidth (LDL) and the corresponding resonant frequency for fork F1 *in vacuo* were
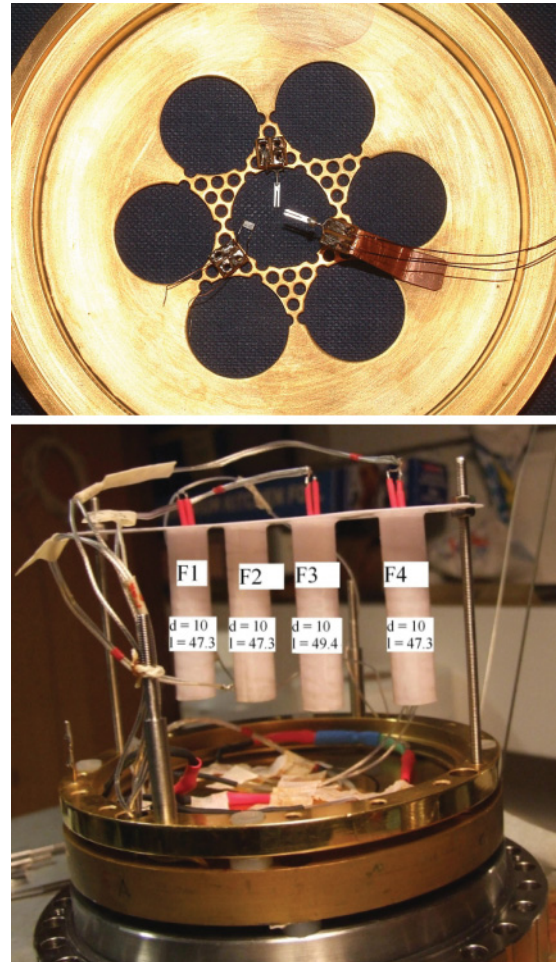

FIG. 1. (Color online) The open experimental cell showing how the forks were mounted. (a) Upper panel, axial view. In the original experiments, the forks were in "free space." Fork f1 (seen on the top) is mounted 1 mm from a grid (not used here) and fork f2 (right) is 11 mm from the grid. An RuO$_2$ temperature sensor is also seen (left), and fork f3 is not visible. (b) Lower panel, side view. In the second set of experiments forks F1, F2, F3, F4 were mounted inside Stycast tubes, positioned as described in the text. The inner diameters d and lengths l of the tubes are indicated in mm.

monitored over many hours with the cell at its base temperature of ∼10 mK, keeping the prong peak velocity at ≈1 cm/s. Although the exact temperature of the fork was unknown, it was low enough for the fork characteristics to have become temperature independent: a subsequent cooling of F1 from room temperature to ∼10 mK with a helium sample present led to a similar change in the fork's center frequency. As shown in Fig. 2(a) for fork F1, both the resonant frequency and the linewidth were highly stable, and the same was true of all the other forks. F4 displayed a vacuum linewidth of a few Hz, probably due to mechanical damage while being mounted, and it was therefore disregarded.

B. Oscillations in He II

The forks' oscillatory behavior in He II at ∼10 mK was markedly different from that *in vacuo*. For low-driving amplitudes, such that the peak velocities of the fork tips were
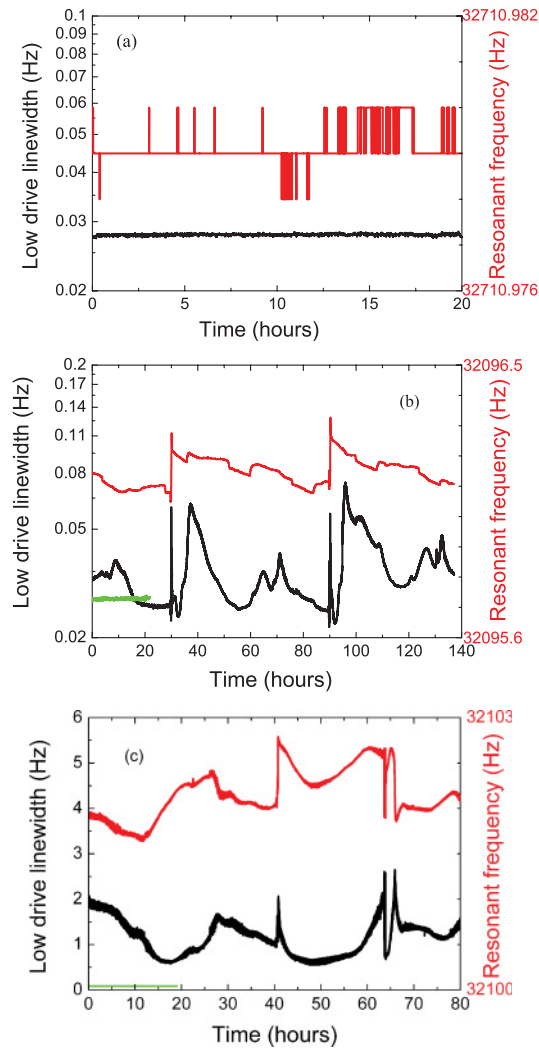
FIG. 2. (Color online) (a) The low-drive linewidth (LDL) of fork F1 measured *in vacuo* at low temperature as a function of time is shown by the lower (black) line and left-hand ordinate, and the corresponding resonant frequency by the upper (red) line and right-hand ordinate. (b) The equivalent plots for F1 in superfluid helium at the base temperature ($\sim$10 mK) of the dilution refrigerator. The jumps observed near 30 and 90 h coincide with the liquid-helium transfers into the main bath. The (green) horizontal line indicates the vacuum LDL. (c) The equivalent plots for f2 where, again, the jumps correspond to helium transfers.

far below that needed for production of what is clearly strong QT (see Sec. IV), we observed three distinctly different kinds of response:

(i) Fork F1 (inside its original encapsulation) exhibited narrow Lorentzian resonances that were accurately reproducible on a time scale of a few tens of minutes, but whose center frequency and low-drive linewidth (LDL) drifted on a time scale of hours. As shown in Fig. 2(b), the drift led to LDLs ranging from 0.07 Hz down to the vacuum linewidth.

(ii) Forks f1–f3 (mounted in "free space") also exhibited Lorentzian resonances. As shown for f3 in Fig. 2(c), they too exhibited drifts in their center frequencies and LDLs on a time scale of hours, but the LDLs were much larger than for F1 and they never fell as low as their vacuum values.
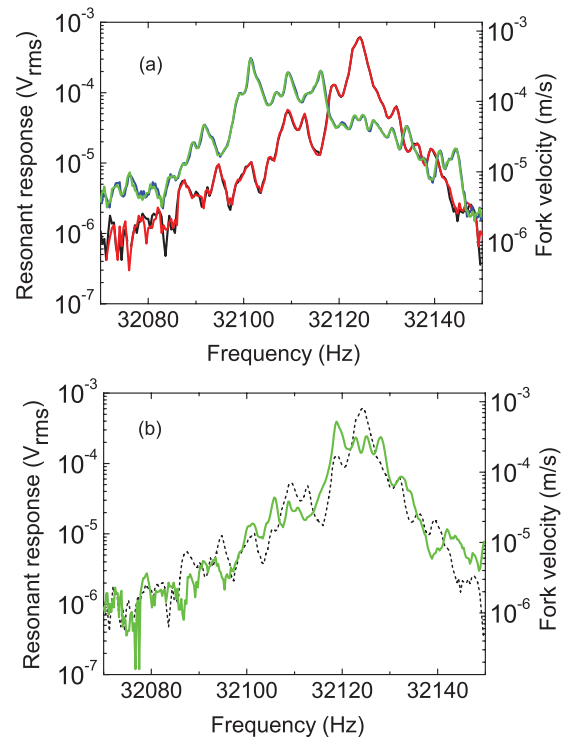

FIG. 3. (Color online) (a) Resonant responses of forks F2 (lower pair of almost coincident curves, black increasing and red decreasing frequency) and F3 (upper pair, green and blue, respectively) in superfluid ^{4}He at $T \sim 10$ mK under 5.0 bar pressure (left-hand ordinate). The corresponding peak fork velocity for F2 is shown on the right-hand ordinate; to find the equivalent velocities for F3, the ordinate numbers should be multiplied by the ratio of the forks' a parameters, $1.06/1.09 = 0.973$. The response on a time scale of tens of minutes is seen to be highly reproducible. (b) Frequency response of F2 with a drive amplitude of 0.97 mV$_{rms}$ on two occasions separated by several hours, measured with helium levels in the main bath of 99.4% and 32.6% (black dashed and full green lines, respectively).

(iii) Forks F2, F3 (bare, in tubes) exhibited the broader, more complex responses shown in Fig. 3(a), behavior that can not be described by a single Lorentzian. As shown in the figure, these complicated responses were accurately reproducible on a time scale of a few tens of minutes, when the same frequency region is scanned back and forth in both directions. Over a longer interval, a change occurred in the detailed shape of the resonance as shown in Fig. 3(b).

We had in mind that acoustic emission from the forks might contribute significantly to the linewidths,[12,13,21] but that this effect might be small in the case of F1 because at its fundamental resonance, the acoustic wavelength of 7.5 mm is much larger than any dimension of the encapsulation. Support for this idea came when we excited F1 near its first overtone. The corresponding resonance, shown in Fig. 4 (right), fell at a frequency $\sim$5.9$\times$ higher than that of the fundamental (a ratio close to the value of $\sim$6.1 found experimentally for much larger tuning forks at room temperature[22]). The associated wavelength was correspondingly reduced to become comparable with the dimensions of the encapsulation. The observed LDL of about 97 Hz was $\sim$3600 $\times$ larger than that at the fundamental (left): it displays complex structure similar to the
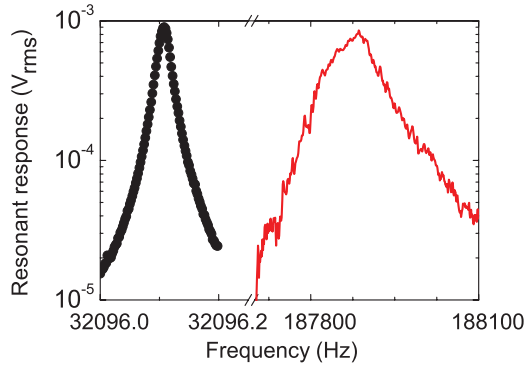
FIG. 4. (Color online) The low-drive frequency response of fork F1 near its fundamental (left side, black filled circles) and first overtone (right side, red line) resonances. Note that the "ripples" on the overtone resonance are not noise, but are accurately reproducible over a time scale of minutes.

fundamental mode responses of F2, F3. On a time scale of a few tens of minutes, the structure was highly reproducible. We discuss acoustic effects further in Sec. V.

We wondered whether the drifts in the LDLs and resonant frequencies of f1–f3 and F1 might be associated with tiny pressure changes due to the variation of the helium level in
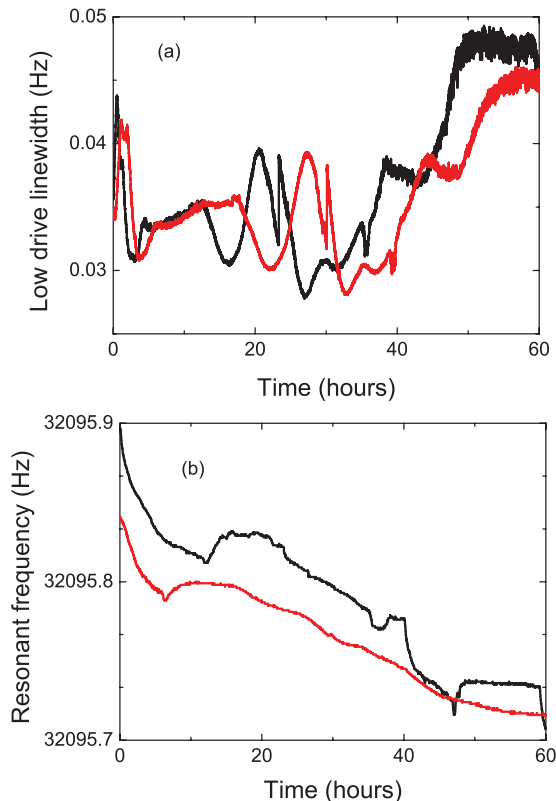

FIG. 5. (Color online) Plots to show the reproducibility of the drift in (a) the low-drive linewidth (LDL) and (b) resonant frequency of fork F1 in superfluid helium at $T \sim 10$ mK as functions of time. Two evolutions are plotted, each spanning the interval during which the level of liquid helium in the main bath fell from maximum to minimum, while the system remained entirely undisturbed. In each case, measurements started from when the helium fill was completed.

the main helium bath (see Sec. V A 3). To test this idea, we followed the LDL and resonant frequency of F1 over two periods of many hours, each starting from a time at which the main bath was filled. During each period, the cryostat was otherwise left completely undisturbed. The time variations of the characteristics on these two occasions are compared directly in Fig. 5. The agreement between the evolutions is not perfect, but the two evolutions are similar, with the main features being reproduced, albeit with offsets in time, thus supporting the idea that drifting LDLs and resonant frequencies are associated with a drifting pressure.

Bearing in mind the existence of the slow time-dependent changes of LDL, and accepting that these are always present and must affect all investigations, we now focus on effects associated with the transition from pure superflow to the regime of turbulent drag.

IV. EXPERIMENTS ON THE TRANSITION TO TURBULENCE

To investigate changes in the fork response associated with vortex creation and any subsequent transition to turbulence, we chose not to use forks F2 or F3 because (i) the complicated multiple resonances would make interpretation difficult; and (ii) their relatively high acoustic dissipation (see below) made these forks insensitive to small amounts of dissipation associated with vortex production.

We display our experimental results for the dependence of drag force F on prong velocity υ in the form of plots of the dimensionless drag coeffficient C_D against υ, the drag coefficient being defined by the equation

$$F = \tfrac{1}{2}\rho A C_D \upsilon^2, \qquad (1)$$

where ρ is the density of the helium, and A is the projected area of the oscillating object on a plane normal to its velocity. In Fig. 6, we show representative results for a number of different forks. The fork F1 has a very small LDL (it is in its original can, except for a very small hole), and we note that especially in this case there are two fairly well-defined critical velocities of $\upsilon_{c_1} \approx 0.6$ cm s^{-1} and $\upsilon_{c_2} \approx 10$ cm s^{-1}. Above the lower critical velocities, C_D remains proportional to $1/\upsilon$, but the constant of proportionality has increased. In the limit of high velocities, C_D for each fork seems to be leveling off at a value of order 0.1, which we interpret as characteristic of fully developed turbulence, although the precise limiting value seems to vary markedly from fork to fork. An interesting feature of fork F1 is the presence of hysteresis (shown most clearly in the inset of Fig. 6): the transition at υ_{c_2} from the laminar to the turbulent drag regime occurs with a sudden jump while increasing the drive in small discrete steps, whereas the transition from turbulent to laminar drag is smooth and continuous when the drive level is being decreased again (cf. behavior observed earlier by Bradley *et al.*[9]).

In Fig. 7 we show for a particular fork (f3) how the drag coefficient changes as the LDL drifts from one value to another. In practice, we waited while the LDL drifted with time until it had reached a chosen value, and then made the measurements. Although for this fork the lower critical velocity is less clear than it is for fork F1, there is clear evidence that between the two critical velocities the factor by which the drag coefficient
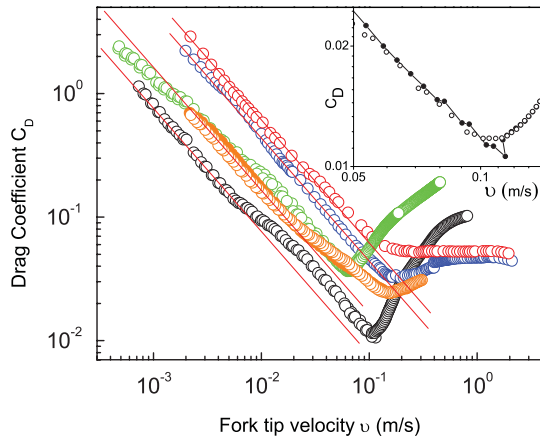
FIG. 6. (Color online) The drag coefficient C_D plotted as a function of peak fork velocity υ for different forks. The lowest set of points (open black circles) are for fork F1. The set of points that correspond to the largest value of C_D at high velocities (open green circles) are taken from Ref. 9 and relate to a pressure of 1 bar; all the other data shown are for $P = 5$ bar. The other three sets of points (red, blue, and orange) all relate to fork f3, for different values of the LDL. The (red) lines indicate a gradient of -1. Inset: a blowup of the region near the minimum for F1, showing evidence for hysteresis. The filled and open points correspond, respectively, to increasing and decreasing velocity.

is changed can be either larger than or smaller than unity; it is larger if the LDL is small, but smaller if the LDL is large.

The results of Fig. 6 show that what are apparently very similar forks can behave in ways that are markedly different, not only at low velocities where, as we shall argue later, the behavior is apparently being influenced by varying acoustic coupling, but also at high velocities where damping due to acoustic coupling is likely to be small relative to that due to turbulent drag. In all cases, the value of C_D does seem to level
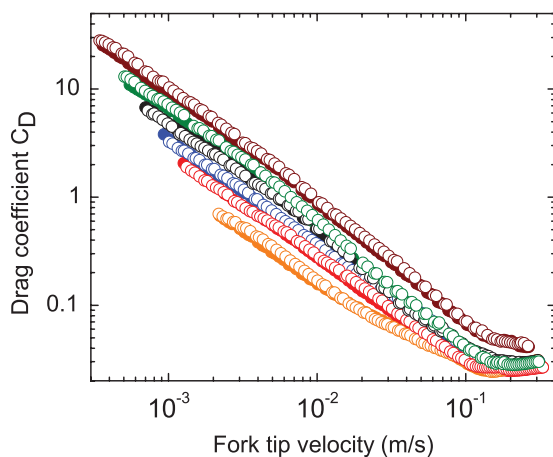

FIG. 7. (Color online) The drag coefficient C_D for f3 plotted as a function of peak fork velocity for $P = 5$ bar, $T \sim 10$ mK, and a range of different initial LDLs: from the bottom, 0.11, 0.18, 0.24, 0.32, 0.48, and 0.76 Hz. In each case, measurements are plotted both for increasing (full circles) and decreasing (open circles) values of the force. The low-temperature vacuum LDL for the same fork was 0.05 Hz.

off to a constant value at high velocities; but while this limiting value varies from fork to fork, it is always significantly less than unity, with perhaps some tendency to be larger when the LDL is small.

V. DISCUSSION

A. Possible mechanisms underlying the low-velocity phenomena

As we mentioned in Sec. I, one might expect that in helium at the lowest temperatures the damping of a fork at low velocities would not exceed that observed *in vacuo*, because potential flow of the helium would exert no drag, although one would expect to see a reproducible reduction in resonant frequency because of a hydrodynamic contribution to the effective mass of a prong. However, in practice, as we have seen, the LDL of a resonance was usually much larger than its value *in vacuo*, and both the LDL and the frequency shift drifted up and down with time.

There are two possible mechanisms that might in principle be responsible for these apparently anomalous effects: processes involving remanent quantized vortices, and acoustic emission from the fork. First, we show that remanent vortices are unlikely to be responsible. Then, we show, first by general arguments and then by detailed calculation, that acoustic emission could well be to blame.

1. Remanent vortices

One factor that is known to change with time in undisturbed He II at very low temperatures is the density of remanent vortices,[23] which typically decreases on a time scale of hours following the creation of lines on passing through T_λ or after some disturbance to the liquid. The drifting LDL might therefore be associated with a configuration of remanent vortices that varies with time. Remanent vortices attached to a fork can contribute to its LDL because oscillations of the prongs of a fork can excite Kelvin waves on these vortices. The resultant energy dissipation could vary with time because the number of attached vortices changes, or because varying boundary conditions at the far ends of the vortices (due to movement of these far ends between pinning centers) modifies the Kelvin-wave resonant frequencies. We can estimate the density of attached vortices required to account for the observed LDLs of up to 2 Hz. The maximum force that a single attached vortex can exert on the prong of a fork is equal to the tension in the vortex which, in general, will have two components, only one of which is dissipative. We assume that it is the latter component that dominates. We also assume that this maximum dissipative force occurs at the critical velocity v_{c1}; if, as is possible, it were to occur at a higher velocity, the minimum density of attached vortices would be larger. A simple calculation then shows a linewidth of 2 Hz requires a minimum density of attached vortices $\sim 4.7 \times 10^{10}$ m^{-2} per unit area of prong, corresponding to a spacing between pinned vortices of about ~ 4.6 μm. More sophisticated calculations give similar results.

We can compare this line density with the maximum density of lines pinned between parallel plates separated by D, estimated by Awschalom and Schwarz[23] as

$$L_R = 2 \ln (D/\xi)/D^2, \qquad (2)$$

where ξ is the vortex core parameter; at any higher density, the vortex lines would disappear by annihilation of lines of opposite sign. Taking as the minimum value of D the minimum spacing between one of the forks and the grid, which is about 1 mm for f1, we find $L_R \sim 3.4 \times 10^7$ m^{-2}, i.e., too small by a factor of ~ 1000 to account for the observed linewidth. Even if we take $D = 0.2$ mm, corresponding to the distance between the prongs, the maximum remanent vortex line density is still too small by a factor of 40 to account for the observations.

This conclusion is consistent with two other observations. First, while it would be easy to understand an LDL that *falls* with time, corresponding to a decreasing remanent vortex density, we can imagine no mechanism that could lead to a spontaneous *increase* in vortex density (Fig. 2). The second is the fact that driving the fork at a velocity that produces fully developed turbulence for a short period has no effect on the LDL: afterward, it resumes its drifting as though nothing had happened. It is hard to believe that the configuration of remanent vortices could remain unaffected by this procedure.

2. Acoustic emission

The other possible source of dissipation is direct sound production by the oscillating fork. Simple calculations, confirmed by detailed investigations using forks of up to 100 kHz, suggest that acoustic energy losses could, in principle, lead to a broadened LDL of the same order as that observed.[12,13,21] Furthermore, we may note that it could in principle provide a plausible explanation of the relative magnitudes of the LDL shifts in the three different fork environments considered in this paper. For fork F1, the LDL broadening is minimal because the fork is still within its own can, the dimensions of which are less than the acoustic wavelength at 32 kHz; for F2, F3, the broadening is very large because their tube radii are such that there are radial mode resonances close to 32 kHz; and for f1, f2, f3 the broadening is relatively small because the forks are far from the walls and internal structures of the cell. We shall make these ideas more quantitative later when we estimate how strongly a fork can couple to the acoustic modes of a cell (Sec. V B). However, this coupling does not in itself explain the drifting with time.

We have considered whether a combination of acoustic emission and remanent vortices could account for the drifting. The emitted sound waves will result in a complicated pattern of nodes and antinodes within the (rather ill-defined) interior structure of the cell. If they were being refracted by the slowly evolving structure of remanent vortices, perhaps it would result in a slowly changing intensity of reflected sound at the position of a given fork, at least in the cases of forks f1, f2, f3? However, an estimate of the acoustic refractive index of a vortex system based on Fetter's phonon-vortex cross section[24] shows that the effect must be small because the scattered amplitude changes sign according to whether the scattering is to the left or to the right (being dependent on $1/\theta$, where θ is the scattering angle). Thus, for a random ensemble of vortices, the refraction will exactly cancel to first order. Although the cancellation will not in fact be exact, the effect of vortices on sound propagation is clearly small, consistent with a calculation[25] of the effect of turbulence on the speed of sound in a classical fluid. The drifting must therefore arise for some other reason.

3. Sensitivity to pressure

We now suggest that the drifting is associated with tiny changes in the velocity of sound due to very small changes in the pressure in the experimental cell. In our experiments, the tube through which the cell is filled with helium passes through the main helium bath and is closed off at the top of the cryostat. Small, slow, changes in pressure in the cell therefore result from the slow fall between fillings in the level of the helium in the main bath. The resultant cyclical (2–3 day) variation in pressure is about 0.02 bar, which would result in a change in the velocity of sound of about four parts in 10^4. We will show below that this would be sufficient to shift the frequency of an acoustic normal mode into or out of resonance with a fork, and therefore to have a strong effect on the damping of the fork.

B. Coupling to acoustic modes

1. Theory based on a model fork

Discussions relating to the emission of sound by a tuning fork into a volume of liquid helium have been presented by Schmoranzer *et al.*,[12] Bradley *et al.*,[21] and Salmela *et al.*[13] Here, we focus on an attempt to provide an explanation of the effects reported above. In essence, a tuning fork in a closed volume of helium is a system in which one simple oscillator, the fork, is coupled to a large number of other simple oscillators, formed from the longitudinal acoustic normal modes in the helium. We shall set up and solve equations that describe this system, and then assess the extent to which these equations can account for our experimental observations.

An accurate treatment of the radiation of sound by a tuning fork is difficult because of its shape. In essence, a small fork must be a quadrupole radiator of sound, and therefore we shall take as the simplest tractable model of the fork an oscillator formed from a pair of spheres subject to elastic restoring forces, such that they can oscillate relative to one another in antiphase along their line of centers with a natural angular frequency ω_0; the spheres are constrained so that there can be no motion perpendicular to the line of centers. Each sphere has a radius a, and their centers are separated by a distance b, where b is comparable with a. If the speed with which the spheres oscillate is $U_0 \exp(-i\omega t)$, the velocity potential produced by the motion of one sphere is that due to two sources forming an oscillating dipole of strength[26]

$$D = 2\pi a^3 U_0. \tag{3}$$

Then, the combination of the two oscillating spheres leads to a velocity potential due to an axial (or longitudinal or linear) quadrupole, the quadrupole moment tensor having an (xx) component given by

$$Q_{xx} = Db, \tag{4}$$

if the two spheres are aligned along the x axis. This simple model of a fork is probably adequate for our purposes provided that all the dimensions of the fork are significantly smaller than the wavelength of the emitted sound, which is the case for the 32-kHz forks with which we are concerned.

The details of our calculations are set out in the Appendix, and they can be summarized as follows. The velocity potential

describing the acoustic radiation from the model fork into an unbounded volume of helium is easily calculated by summing the Green's functions that describe the radiation from each of the four point sources to which the quadrupole is equivalent. To take account of reflections from the walls of a containing vessel, we recognize that the sound field in this vessel generated by the oscillating quadrupole must be expressible as a superposition of normal modes, with frequencies ω_n. The fact that there is a large acoustic mismatch between the helium and the walls of the vessel ensures that these modes are lightly damped. The appropriate Green's functions must then be expanded in terms of these normal modes. It follows that each normal mode responds to the vibrating fork as though it were an oscillator with natural frequency ω_n driven at the frequency ω of the fork, and the appropriate coupling constants are calculated in the Appendix. Suppose that only one normal mode is close in frequency to the fork frequency, so that only this mode is excited with significant amplitude by the vibrating fork. Let $\bar{\Phi}_n$ be the amplitude of the velocity potential associated with this mode averaged over the volume V of the cell in which the fork is placed, and let ξ be the amplitude of oscillation of one of the spheres in our model fork. Taking into account the coupling to the fork, we find that the equation of motion of this mode is

$$\omega_n^2 \bar{\Phi}_n - i\omega\mu_n \bar{\Phi}_n - \omega^2 \bar{\Phi}_n - i\beta_n \omega \omega_n^2 \xi = 0, \qquad (5)$$

where μ_n describes the natural damping of the acoustic mode, and where

$$\beta_n = 2\pi a^3 b \frac{\zeta_n}{V} \cos^2\theta. \qquad (6)$$

θ is the angle between the line joining the two spheres of the model fork and the direction of the wave vector of the nth acoustic normal mode at the position of the fork; ζ_n is the factor by which the amplitude of this acoustic mode at the position of the fork differs from its average amplitude $\bar{\Phi}_n$; and μ_n describes the natural damping of the nth acoustic mode. The fork is coupled to the acoustic mode because the fluid velocity in this mode exerts an inertial force on the fork. Taking this force into account, we find that the equation of motion of the fork is

$$\omega_0^2 \xi - i\omega\mu_0 \xi - \omega^2 \xi + i\gamma_n \omega \omega_n^2 \bar{\Phi}_n = f_0, \qquad (7)$$

where the vibrations of the fork are supposed to be externally driven by a force f_0, μ_0 describes the natural damping of the fork, and

$$\gamma_n = \frac{(C+1)\rho b}{c^2 \rho_0} \zeta_n \cos^2\theta. \qquad (8)$$

The parameter C is equal to 0.5 for our model fork, ρ is the density of the helium, and ρ_0 is the density of the material of the fork.

Solution of Eqs. (5) and (7) yields the response of the fork to the drive f_0, when coupling to the nth acoustic mode is taken into account:

$$\frac{\xi}{f_0} = \frac{\omega_n^2 - \omega^2 - i\omega\mu_n}{\left(\omega_0^2 - \omega^2 - i\omega\mu_0\right)\left(\omega_n^2 - \omega^2 - i\omega\mu_n\right) - \beta_n \gamma_n \omega^2 \omega_n^4}. \qquad (9)$$

2. Comparison with experiment: Forks in an open geometry

We now use Eq. (9) to explore how a real fork might be expected to behave in the relatively open geometry provided by the 1.5 ℓ pressure vessel. The model fork might be expected to behave similarly to that of a real one if we take a to be something like the width of a prong and b to be the separation between the centers of the two prongs. Typically, then we can take $a = 0.35$ mm and $b = 0.8$ mm. We choose these particular values so that the predicted acoustic power radiated by our model fork is equal to that radiated by the model fork analyzed by Schmoranzer *et al.* [their Eq. (3b)], which took greater account of the detailed shape of a real fork. For a 32-kHz fork, the angular frequency $\omega_0 = 2 \times 10^5$ s^{-1}. We take $\rho = 152$ kg m^{-3} and $c = 273$ m s^{-1} for a pressure of 5 bar. We take the density ρ_0 to be that of quartz, which is 2700 kg m^{-3}, $C = 0.5$, $\cos^2\theta = 0.5$, and $V = 1.5 \times 10^{-3}$ m^{-3}. Tentatively, we shall assume that the amplitude of the relevant acoustic normal modes is roughly constant over the volume of the pressure cell, so we assume that $\zeta_n = 1$. We shall also need estimates of the damping coefficients μ_0 and μ_n. The vacuum linewidth (FWHH) for a tuning fork is typically 0.02 Hz, which yields a value of μ_0 of 1.26×10^{-1} s^{-1}. The bulk attenuation of sound at a frequency of 32 kHz is very small at the low temperatures with which we are concerned, so that the damping of an acoustic mode in the pressure cell is probably due largely to imperfect reflection at the walls of the cell and at various obstacles inside the cell. Expressing this reflection coefficient in terms of the acoustic impedances of the helium and of the walls, etc., of the cell (assumed to be copper) leads to an estimated $\mu_n \simeq 40$ s^{-1}. Hence, we estimate $\beta_n = 7.18 \times 10^{-11}$ m, and $\gamma_n = 4.53 \times 10^{-10}$ m^{-1} s.

We show in Fig. 8(a) plots of the response, $z_1(\Delta\omega, \omega_n) = |\xi/f_0|$, given by Eq. (9) against the detuning from resonance $\Delta\omega = \omega - \omega_0$, for different values of the frequency ω_n of the nth acoustic normal mode. We see that when ω_n is close to ω_0, the linewidth of the response is greatly broadened, although the response remains more-or-less Lorentzian. There are also small shifts, of order the linewidth, in the resonant frequency.

To make further progress, we need some information about the normal acoustic modes in the volumes of superfluid helium with which we are concerned. Consider first the situation when a fork is situated in the open volume within the 1.5 ℓ pressure vessel. This vessel contains structures that are complicated in shape, and it is therefore impracticable[13] to derive any detailed information about the normal modes. However, the volume is quite large, so that its linear dimensions are large compared with the wavelength of the sound generated by a fork. In these circumstances, we can at least calculate the density of states associated with the normal modes, which depends only on the volume, and hence obtain a good estimate of the spacing in frequency between these modes. The number of modes in volume V with angular frequency in the range $d\omega$ is given by

$$n(\omega) = \frac{V}{2\pi^2 c^3} \omega^2 d\omega, \qquad (10)$$

so that the relative spacing between modes is

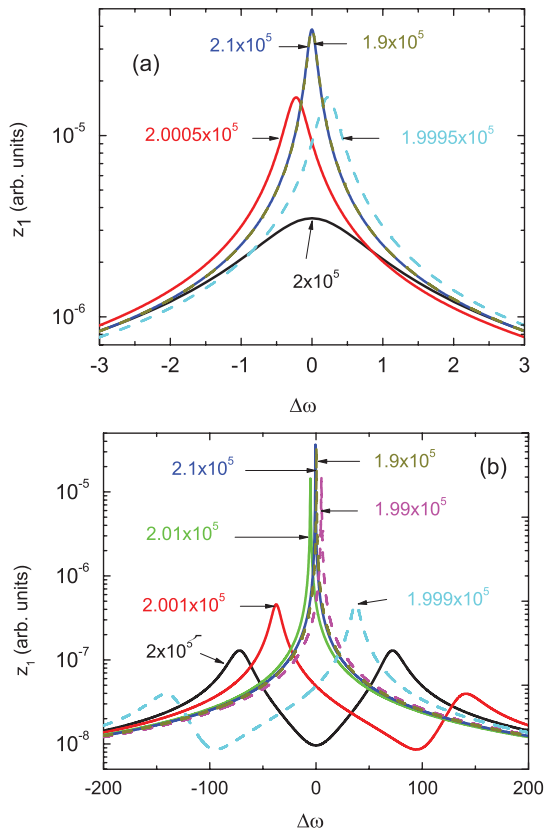$$\frac{\delta\omega}{\omega} = \frac{2\pi^2 c^3}{V\omega^3}. \qquad (11)$$

FIG. 8. (Color online) (a) Plots of z_1 against $\Delta\omega$, for different values of the frequency ω_n (given by the number against each curve), with coupling parameters $\beta_n = 7.18 \times 10^{-11}$ m and $\gamma_n = 4.53 \times 10^{-10}$ m^{-1} s. (b) As in (a) but with $\beta_n = 1.44 \times 10^{-9}$ m and $\gamma_n = 9.06 \times 10^{-9}$ m^{-1} s.

Thus, at a frequency of 32 kHz in a volume of 1.5 ℓ, the spacing between modes is 1.05 Hz. Not all these modes will couple strongly to the fork, but a substantial fraction are likely to do so. More precisely, as we have already assumed, all the relevant modes are taken to have an approximately constant amplitude over the volume of the pressure vessel. Thus, if the pressure in the cell drifts in such a way that the speed of sound in the helium changes by only 1 part in 3×10^4, it is very likely that the frequency of a well-coupled acoustic mode will come close to that of the fork, resulting in a substantial increase in the fork's linewidth of the fork response and a small shift in its resonant frequency. This is in accord with the experimental results described above. Exact numerical agreement can not be expected, partly because of the relatively crude nature of our model, and partly because of uncertainties in the numerical values of the various parameters.

3. Comparison with experiment: Forks in a confined geometry

So far, we have focused on the behavior of a fork in the relatively open geometry of our 1.5 ℓ pressure vessel. For fork F1, still enclosed within its original can (with a very small hole), the LDL drift was greatly reduced. It is reasonable to suppose that this was due to reduced coupling with the acoustic modes in the pressure vessel. However, when a fork, without its can, was placed inside one of the open ended tubes, the single resonance was replaced by multiple resonances, separated by

1–2 Hz and extending over a frequency range of about 80 Hz (Fig. 3). We need to discuss how this very different type of behavior might arise. We remark that the close separation of these resonances suggests strongly that coupling to the acoustic modes of the 1.5 ℓ pressure vessel is still involved; the modes associated with the open-ended tubes are much more widely spaced.

Simple broadening of the fork resonance, accompanied by a small shift in resonant frequency, illustrated in Fig. 8(a), is predicted to occur only for values of the coupling parameters β_n and γ_n similar to those that we have used. If these coupling parameters were to be significantly larger, then our equations lead to a different behavior, as shown in Fig. 8(b). When the frequencies ω_0 and ω_n are within a few mode spacings of each other, the single resonant peak can be replaced by two peaks, separated in frequency by much more than the acoustic mode spacing. Figure 8(b) takes into account only one acoustic mode; if we take into account the fact that there are many acoustic modes, separated in frequency by about 1 Hz and with different coupling parameters, the resultant overall response might very well be similar to that shown in Fig. 3.

The form of coupling parameters given by Eqs. (6) and (8) implies that the required increase in these parameters, when the forks are enclosed in the open-ended tubes, could result from an increase, by ~ 20 in the amplitude of each normal mode inside the open-ended tube, relative to its amplitude outside the tube. Here, we are thinking in terms of the normal modes of the whole volume of helium (both inside and outside the tube).

Let us for a moment think in terms of two separate volumes of helium: the volume inside the tube and that outside the tube. And let us first ignore the coupling between them. The volume inside the tube has a simple shape, so that we can easily calculate its normal modes. We use cylindrical polar coordinates r, ϕ, z; the closed end of the tube is at $z = 0$; the open end at $z = h$; the inner surface of the tube is at $r = R$. The velocity potential for the normal modes has the form

$$\Phi_{k_q, m, k_z} = J_m(k_q r) \exp(im\phi) \exp(ik_z z) \exp(-i\omega t), \quad (12)$$

where $k_q^2 + k_z^2 = \omega^2 / c^2$. The boundary conditions are that the $\partial\Phi/\partial r = 0$ at $r = R$, $\partial\Phi/\partial z = 0$ at $z = 0$, and $\Phi = 0$ at $z = h$. A fork placed on the axis of the tube will couple only to modes with $m = 2$. The lowest such mode, if $k_z = (2n + 1)\pi/2h$, and $n = 6$, has a frequency equal to 32.66 kHz, where we have taken $R = 5$ mm and $h = 47.1$ mm. Given that R is not known very precisely, we see that this mode could well have a frequency very close to that of a fork. In reality, this ("inside") mode is coupled to acoustic modes of the helium outside the tube ("outside" modes), and the true normal modes of the whole volume of helium include such coupled modes. Now consider the coupled modes formed from the "inside" mode at 32.66 kHz and an "outside" mode at a slightly higher or lower frequency. There are two such modes, one of which has a large amplitude inside the tube and a small amplitude outside the tube, the other of which has these amplitudes reversed. The first of these has just the property we need to obtain enhanced values of β_n and γ_n. We have not attempted to put these ideas on a proper quantitative footing, but we submit that they could well account for the behavior seen in Fig. 3(a).

It is interesting to note that the forks studied by Schmoranzer *et al.*[12] seemed, even in an open geometry, always to exhibit a response similar to our forks F2 and F3, which were enclosed in the open-ended tubes. However, the vessel in which the former forks were situated was smaller in volume by a factor of about 240 than our 1.5 ℓ pressure cell, and the former forks were also of a higher natural frequency (77 or 100 kHz). This means that the coupling parameters were much larger than ours, so the difference in behavior is in fact not unexpected.

C. Transition to turbulence

Having confirmed the likely role of coupling to acoustic modes, we now discuss our data on the transition from potential flow of the pure superfluid to quantum turbulence. First, we recall the behavior of an oscillating structure in a classical fluid and, in particular, that of a tuning fork. Recent investigations[3] have shown that forks in a classical fluid behave very much as expected. At low velocities, the fork experiences a linear viscous drag, giving rise to a drag coefficient

$$C_{\mathrm{D}} = 2\alpha \frac{S}{A} \sqrt{\omega \nu} \, \frac{1}{\nu} \, , \qquad (13)$$

where ν is the kinematic viscosity of the fluid, and $\alpha \sim 1$ depends on the exact shape of the fork.[27] This form is applicable when, as here, the viscous penetration depth is small compared with the dimensions of a prong. As the velocity is increased through the transition to turbulence, C_{D} decreases less rapidly, tending at large velocities to a value very close to unity. Within the transition region, the drag coefficient exhibits no special features, and no precise critical velocity can be identified. Visualization of the flow suggests that the initial instability may involve the production of Taylor-Görtler vortices in the viscous penetration depth near the corners of the prong, but the complicated sequence of processes leading to fully developed turbulence is not known.

The transition to turbulence in a pure superfluid in the zero-temperature limit must be fundamentally different because it involves a transition from potential flow with complete slip at a boundary, rather than from laminar viscous flow. In fact, potential flow can only be an approximation because the QT must be nucleated from remanent vortex lines. The experiments show that there is still a regime at the smallest velocities where $C_{\mathrm{D}} \sim 1/\nu$, but this must be associated with a linear damping of the motion of the fork from internal friction or acoustic radiation. At high velocities, C_{D} does seem still to tend to a constant value, albeit one that seems not to be reproducible from fork to fork, and it usually seems to be much less than unity. At intermediate velocities, the drag coefficient often goes through a sharp minimum, which we can identify with the critical velocity ν_{c_2}, although again the details vary from fork to fork. For the moment, we ignore the lower critical velocity ν_{c_1}.

Measurements of C_{D} for similar forks in superfluid ^{4}He above 1 K (Ref. [4]) showed that, as the temperature was lowered below the T_λ, the form of C_{D} evolves from that characteristic of a fork in a classical fluid toward that involving a sharp minimum, followed sometimes by a broad maximum, before leveling off at a value in the range 0.5 to 1. This led

Blazkova *et al.*[4] to point out that the transition to turbulence had features similar to those in a classical fluid, and this idea was incorporated into a semiempirical formula that described quite well the detailed form of C_{D} in the transition region. However, the required fitting parameters varied from fork to fork in a way that was not understood. According to the empirical formula, the sharp minimum in C_{D} marks the onset of a rapid production of vortex line; the resulting high density of vortex line in the neighborhood of the fork leads to a strong coupling between the two fluids, which then behave like a single classical fluid undergoing a transition to turbulence closely similar to that occurring in a classical fluid.

Comparing the observed behavior of the forks above 1 K with that at the much lower temperatures used here, we see that, although the broad features are similar, the degree to which different forks differ in behavior seems to be more marked at the lower temperatures, and that the limiting value to which the drag coefficient tends at high velocities seems to be significantly smaller. The empirical formula can still be fitted to the data at very low temperatures (although the drag at low velocities must now be attributed to internal damping and acoustic emission), but the fitting parameters vary more widely from fork to fork. We note in passing that Bradley *et al.*[9] obtained a better fit to a slightly different empirical formula, but its parameters were observed to change greatly when the same fork was placed in a different cell; the change was tentatively attributed to an accumulation of dirt on the fork. Part of this change, especially that at low drives, may have been due to a change in acoustic emission: their cells were smaller than our pressure cell and contained a large volume of silver sinter. We might therefore expect the effects of acoustic emission to be different from those we have observed.

Two conclusions can be drawn. The fact that the limiting value of C_{D} at high velocities seems to be much smaller than unity at low temperatures suggests that the turbulence is becoming less classical in character as the temperature is reduced; and the fact that different, but apparently very similar, forks behave in different ways suggests that the form of the turbulence generated by a fork depends on very minor differences between forks that are hard to identify. Of course, this sensitivity may be characteristic of quantum turbulence, and it may mean that the details of the processes by which quantum turbulence is nucleated remain important even when the turbulence is fully developed. The suggestion by Bradley *et al.*[9] that an accumulation of dirt on a fork might be important needs to be borne in mind, but it seems to us unlikely that this is generally the case. The recent observation that the turbulent regime associated with an oscillating structure at low temperature is unstable even at the highest velocities[28] may be relevant to the possibility that QT can be very sensitive to minor perturbations.

D. An additional critical velocity

So far, we have been concerned only with the critical velocity ν_{c_2}, associated with the transition to fully developed turbulence. At the other critical velocity ν_{c_1}, well below ν_{c_2}, the drag can either increase or decrease by a small factor, with the sign of the change dependent on the magnitude of the LDL at the time of the measurement. The nature of the change in
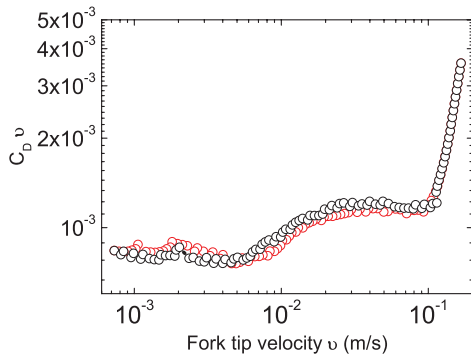
FIG. 9. (Color online) The drag coefficient multiplied by peak velocity $C_D \times \upsilon$ as a function of velocity for fork F1 at 5 bar (replotted from Fig. 6). The scan for increasing velocity is shown by (black) circles and that for decreasing velocity by (red) circles. During the initial decrease from the highest velocity, the data points are coincident.

C_D at this lower critical velocity can be seen more clearly by plotting the product of C_D and velocity against velocity, as shown in Fig. 9 for a case where the drag increases at υ_{c_1}. These data, replotted from Fig. 6, were recorded under particularly stable conditions: although the results are influenced slightly by the drifting LDL, the product υC_D seems to rise from its low-drive constant value to a higher constant value, indicating that there has been a change in the linear damping of the fork.

Effects that set in at a velocity below that at which fully developed turbulence is believed to start to form (υ_{c_2}) have been observed in other experiments with oscillating structures at very low temperatures. Bradley *et al.*[9] found evidence for a sharp increase in the damping of tuning forks at $\sim 0.9\upsilon_{c_2}$. In their work[29] on vibrating wires, they found evidence for a similar increase in damping at about $0.5\upsilon_{c_2}$. Nichol *et al.*[14,30] observed an increase in the effective mass of a vibrating grid, with no measurable change in damping, at a velocity of about $0.1\upsilon_{c_2}$; in subsequent experiments with different grids, the effect seemed either to be absent[15] or[18] to arise at $\sim 0.3\upsilon_{c2}$. A possible explanation of such effects was proposed[31] in terms of the evolution of remanent vortices in an oscillatory flow.

The physics underlying the semiempirical formula[4] implies that, below υ_{c_2}, the fork might be surrounded by an array of vortex lines that allow the superflow to mimic classical laminar viscous flow, resulting in increased damping. Perhaps this type of "viscous flow" sets in at the critical velocity υ_{c_1}? The magnitude of the additional damping might be expected to correspond to that from a classical fluid with kinematic viscosity equal to the minimum kinematic eddy viscosity associated with a tangle of vortices, which is roughly equal to the quantum of circulation. This would be too large to correspond to the extra damping observed above υ_{c_1}, but our estimate of its magnitude could be seriously in error.

The sign of the change in damping at υ_{c_1} can become negative when the LDL is large. If a large LDL is caused indeed by acoustic emission, we might argue that υ_{c_1} has nothing to do with vortex production. However, this is not necessarily the case. The existence of a sheath of vortex lines around the vibrating fork would modify the flow in the superfluid (it would no longer be purely potential), in turn reducing the acoustic

emission. If the resultant damping is reduced by a factor greater than that by which the "viscous damping" is increased, then the overall damping will be seen to have decreased. Obviously, this discussion of possible mechanisms underlying the critical velocity υ_{c_1} is speculative, and we currently have no way of testing the underlying ideas.

VI. CONCLUSIONS

We can draw a number of conclusions.

(i) In using quartz tuning forks for some of the purposes mentioned in Sec. I, one must bear in mind that the size and geometry of their surrounding environment can exert a huge influence on their properties and, in particular, on the line shape and center frequency of their resonances. We have presented compelling evidence that this sensitivity to the surroundings results from coupling to standing-wave acoustic modes. This effect can be substantially reduced by leaving the fork within its own original encapsulation (as with F1) with a small hole bored to admit liquid helium. However, even F1 exhibited pronounced drift in both linewidth and resonant frequency, attributable to there still being a finite coupling to the acoustic modes in the main part of the cell; there may also be some coupling through the walls of the encapsulating can. Both of these effects could probably be reduced by appropriate design.

(ii) Closely associated with this first conclusion, the resonant properties of a typically mounted fork change markedly with tiny pressure variations, e.g., those due to variations in the height of the liquid in the main bath surrounding a filling capillary. Considerable caution should therefore be exercised when using a fork as a pressure sensor.

(iii) Although the transition to fully developed turbulence around forks in superfluid ^{4}He above 1 K has features similar to its classical counterpart, such quasiclassical behavior becomes less evident at lower temperatures.

(iv) Seemingly very similar forks often behave quite differently in their transitions to turbulence, especially at low temperatures, indicating that their behavior is strongly influenced by physical features that appear at first sight to be minor.

(v) There is growing evidence that the transition to fully developed turbulence is preceded at a significantly lower velocity by some other transition, the nature of which remains unclear.

APPENDIX: THE COUPLING OF A MODEL FORK TO ACOUSTIC MODES

We are interested ultimately in the velocity potential generated by our model fork when it is placed in a closed vessel of superfluid helium, at the walls of which a sound wave

is almost completely reflected. This velocity potential can be regarded as being generated by a set of oscillating sources. To clarify our presentation, we first calculate the velocity potential due to a set of point sources in free space, and only after that do we treat the case where the point sources are in a closed vessel.

Consider the velocity potential generated by point sources $S(\mathbf{r}_i)$ in a fluid in free space, each oscillating in time as $\exp(-i\omega t)$. We introduce the Green's function

$$g_\omega(\mathbf{r}|\mathbf{r}_0) = -\frac{1}{4\pi R}\exp(ikR), \qquad (A1)$$

where $R^2 = (\mathbf{r} - \mathbf{r}_0)^2$ and $k = \omega/c$; $g_\omega(\mathbf{r}|\mathbf{r}_0)$ satisfies

$$\nabla^2 g_\omega(\mathbf{r}|\mathbf{r}_0) + k^2 g_\omega(\mathbf{r}|\mathbf{r}_0) = -\delta(\mathbf{r} - \mathbf{r}_0). \qquad (A2)$$

Then, our required velocity potential at the point $\mathbf{r}$ is given by

$$\Phi(\mathbf{r}) = \Sigma_{\mathbf{r}_i} S(\mathbf{r}_i)g(\mathbf{r}|\mathbf{r}_i)\exp(-i\omega t). \qquad (A3)$$

We apply this formula to a dipole, formed from sources $+S$ and $-S$ on the x axis at $x = \pm d/2$, and to a quadrupole, formed from two of these dipoles with their centers at $x = \pm b/2$. For the dipole, the potential at a distance r from the dipole is given by[26]

$$\Phi(r) = -i\frac{kD}{4\pi r}\frac{x}{r}\left(1 + \frac{i}{kr}\right)\exp(ikr - i\omega t), \qquad (A4)$$

where $D = Sd$ is the strength of the dipole, and x is the projection of r onto the x axis. Similarly, the potential due to the quadrupole is easily shown to be given by

$$\Phi(r) = -\frac{k^2 Q_{xx}}{4\pi r}\left[\frac{x^2}{r^2} + \frac{3x^2 - r^2}{r^2}\left(\frac{i}{kr} - \frac{1}{k^2 r^2}\right)\right]$$
$$\times \exp(ikr - i\omega t), \qquad (A5)$$

where $Q_{xx} = Db$.

We turn now to the velocity potential generated by a set of point sources, oscillating at angular frequency ω, in a closed container of superfluid helium. We suppose to start with that sound is reflected perfectly from the walls of the container and suffers no attenuation in the helium. First we seek, for a single source, a solution to the equation

$$\nabla^2 G_\omega(\mathbf{r}|\mathbf{r}_0) + \frac{\omega^2}{c^2}G_\omega(\mathbf{r}|\mathbf{r}_0) = -\delta(\mathbf{r} - \mathbf{r}_0), \qquad (A6)$$

subject to the boundary conditions imposed at the inner surface of the container (normal component of velocity vanishes). Following standard procedures,[26] we express G_ω in terms of the acoustic normal modes of the helium in the container, given by solutions of

$$\nabla^2 \Phi_n + K_n^2 \Phi_n = 0, \qquad (A7)$$

subject to the boundary condition on the normal component of the velocity; the normal modes satisfy orthogonality/normalization conditions, which we write as

$$\int \Phi_n(\mathbf{r})\Phi_m(\mathbf{r})dV = V\bar{\Phi}_n^2\delta_{mn}. \qquad (A8)$$

The integration is over the volume V of the container, and $\bar{\Phi}_n$ is the root-mean-square amplitude of the nth normal mode.

We expand $G_\omega(\mathbf{r}|\mathbf{r}_0)$ in Eq. (A6) in terms of the normal modes

$$G_\omega(\mathbf{r}|\mathbf{r}_0) = \sum_n g_n(\mathbf{r}_0)\Phi_n(\mathbf{r}) \qquad (A9)$$

and use Eq. (A7), obtaining

$$\sum_n g_n(\mathbf{r}_0)\left(\frac{\omega^2}{c^2} - K_n^2\right)\Phi_n(\mathbf{r}) = -\delta(\mathbf{r} - \mathbf{r}_0). \qquad (A10)$$

We multiply by $\Phi_m(\mathbf{r})$, integrate over V, and use the orthogonality condition, so obtaining

$$g_m(\mathbf{r}_0)\left(\frac{\omega^2}{c^2} - K_m^2\right)V\bar{\Phi}_m^2 = -\Phi_m(\mathbf{r}_0). \qquad (A11)$$

Therefore,

$$G_\omega(\mathbf{r}|\mathbf{r}_0) = \sum_m \frac{\Phi_m(\mathbf{r})\Phi_m(\mathbf{r}_0)}{V\bar{\Phi}_m^2\left[K_m^2 - (\omega^2/c^2)\right]}. \qquad (A12)$$

We see that, as expected, the acoustic system behaves as an assembly of independent harmonic oscillators with frequencies $\omega_m = cK_m$, coupled to the single source at $\mathbf{r}_0$. The response due an assembly of such sources is obtained by adding together their individual responses.

We are now able to calculate the velocity potential generated by a quadrupole of the type described above, oscillating in a closed container: four sources positioned along the x axis, forming two dipoles, each of strength Sd, the centers of the two dipoles being separated by b. We see immediately that the velocity potential at a point $\mathbf{r}$ is equal to

$$\Phi(\mathbf{r},\mathbf{r}_0) = Sc^2\sum_m \frac{\Phi_m(\mathbf{r})\mathbf{b}\cdot\nabla_{r_0}\mathbf{d}\cdot\nabla_{r_0}\Phi_m(\mathbf{r}_0)}{V\bar{\Phi}_m^2\left(\omega_m^2 - \omega^2\right)}\exp(-i\omega t),$$
$$\qquad (A13)$$

where $\mathbf{d} = (d,0,0)$ and $\mathbf{b} = (b,0,0)$. Suppose now that only one normal mode (with $m = n$) is close to resonance, and that, in the immediate neighborhood of the quadrupole, $\Phi_n(\mathbf{r})/\bar{\Phi}_n$ has the form

$$\frac{\Phi_n(\mathbf{r})}{\bar{\Phi}_n} = \alpha_1\sin[\mathbf{k}_n\cdot(\mathbf{r} - \mathbf{r}_0) + \psi_1], \qquad (A14)$$

where $|\mathbf{k}_n| = K_n$. Then, we find that

$$\Phi(n,\mathbf{r},\mathbf{r}_0) = -\frac{\omega_n^2 Q_{xx}\cos^2\theta\,\Phi_n(\mathbf{r})\Phi_n(\mathbf{r}_0)}{V\bar{\Phi}_n^2\left(\omega_n^2 - \omega^2\right)}\exp(i\omega t), \qquad (A15)$$

where θ is the angle between the vector $\mathbf{k}_0$ and the axis of the quadrupole, and where $\omega_n = cK_n$ is the natural frequency of the nth normal mode.

We can now apply this result to our model fork, for which $Q_{xx} = 2\pi a^3 bU_0$:

$$\Phi(n,\mathbf{r},\mathbf{r}_0) = -\frac{2\pi a^3 bU_0\omega_n^2\cos^2\theta\,\Phi_n(\mathbf{r})\Phi_n(\mathbf{r}_0)}{V\bar{\Phi}_n^2\left(\omega_n^2 - \omega^2\right)}\exp\left(-i\omega t\right). \qquad (A16)$$

As we have explained, the fork and an excited normal mode form a pair of coupled oscillators. To understand the dynamical behavior of these coupled oscillators, we need to write down an equation of motion for each oscillator, each such equation

containing a term that couples to the other oscillator. We shall write the equation of motion for the excited acoustic normal mode in terms of its root-mean-square amplitude $\bar{\Phi}(n,\mathbf{r}_0)$. Averaging Eq. (A16) over the position $\mathbf{r}$, and rearranging, we obtain for one of our equations of motion

$$-\omega^2 \bar{\Phi}(n,\mathbf{r}_0) + \omega_n^2 \bar{\Phi}(n,\mathbf{r}_0) - 2\pi i a^3 b \omega \omega_n^2 \cos^2\theta \frac{\zeta_n}{V}\xi = 0,$$
(A17)

where $\xi = U_0/(-i\omega)$ is the oscillation amplitude of one of the spheres, and $\zeta_n = \Phi_n(\mathbf{r}_0)/\bar{\Phi}_n$. We emphasize that the ratio ζ_n is independent of the amplitude of the excited mode, so that Eq. (A17) is linear in the two "displacements" $\bar{\Phi}_n$ and ξ.

In a linear approximation, appropriate in our case, the force acting on a solid object of volume V_0 traveling with velocity $\mathbf{U}$ in an ideal fluid of density ρ, moving locally with velocity $\mathbf{u}$, is given by[32]

$$\mathbf{F} = (C+1)\rho V_0 \dot{\mathbf{u}} - C\rho V_0 \dot{\mathbf{U}},$$
(A18)

where the constant C depends on the shape of the object and is equal to $1/2$ for a sphere. In our case, the two spheres can oscillate only in antiphase. Therefore, the first term on the right-hand side of (A18) gives rise to a motion of the spheres only to the extent that the value of the velocity $\mathbf{u}$ at one sphere is different from that at the other. The equation of motion of one sphere, when driven by a force $f_0 \exp{(-i\omega t)}$, can thus be written as

$$-\omega^2 \xi + \omega_0^2 \xi$$
$$= \frac{(C+1)\rho V_0}{M_0}(-i\omega)\mathbf{b} \cdot \nabla_{\mathbf{r_0}}[\hat{\mathbf{b}} \cdot \nabla_{\mathbf{r}} \Phi(n,\mathbf{r},\mathbf{r}_0)]_{\mathbf{r}=\mathbf{r}_0}$$
$$+ \frac{C\rho V_0}{M_0}\omega^2 \xi + f_0,$$
(A19)

where M_0 is the mass of one sphere, and $\hat{\mathbf{b}}$ is a unit vector parallel to $\mathbf{b}$. We have ignored the force on one sphere due to

the velocity field generated by motion of the other sphere; this force merely changes the natural frequency ω_0. Again, making use of Eq. (A14), we find that

$$\mathbf{b} \cdot \nabla_{\mathbf{r_0}}[\hat{\mathbf{b}} \cdot \nabla_{\mathbf{r}} \Phi(n,\mathbf{r},\mathbf{r}_0)]_{\mathbf{r}=\mathbf{r}_0} = bk_n^2 \cos^2\theta \zeta_n \bar{\Phi}(n,\mathbf{r}_0).$$
(A20)

Furthermore, $M_0 = \rho_0 V_0$, where ρ_0 is the density of the sphere material. Thus, (A19) becomes

$$-\omega^2 \xi + \omega_0^2 \xi - \frac{C\rho}{\rho_0}\omega^2 \xi$$
$$+ i\frac{(C+1)\rho b}{\rho_0}\frac{\omega\omega_n^2}{c^2}\cos^2\theta \zeta_n \bar{\Phi}(n,\mathbf{r}_0) = f_0.$$
(A21)

We note that the factor $C\rho/\rho_0$ in the third term of Eq. (A21) is small compared to unity. Its effect is to produce a small shift in the natural resonant frequency of oscillation of the spheres due to the change in effective mass when a sphere moves in an inviscid fluid, and also small shifts in the coupling and forcing terms. For simplicity, and because our model of the fork is quite crude, we neglect it. We make the substitutions

$$\beta_n = 2\pi a^3 b \frac{\zeta_n}{V}\cos^2\theta,$$
(A22)

$$\gamma_n = \frac{(C+1)\rho b}{c^2 \rho_0}\zeta_n \cos^2\theta.$$
(A23)

We now take account of intrinsic damping of the oscillating spheres and acoustic modes by adding to our equations of motion the dissipative terms $-i\omega\mu_n\bar{\Phi}_n$ and $-i\omega\mu_n\xi$, yielding

$$-\omega^2 \xi - i\omega\mu_0\xi + \omega_0^2 \xi + i\gamma_n\omega\omega_n^2\bar{\Phi}_n = f_0,$$
(A24)

$$-\omega^2 \bar{\Phi}_n - i\omega\mu_n\bar{\Phi}_n + \omega_n^2\bar{\Phi}_n - i\beta_n\omega\omega_n^2\xi = 0.$$
(A25)

These are our final equations describing the coupled motion of the model fork and nth normal acoustic mode of the helium in the enclosing cell.

---

[1] R. Blaauwgeers, M. Blazkova, M. Clovecko, V. B. Eltsov, R. de Graaf, J. Hosio, M. Krusius, D. Schmoranzer, W. Schoepe, L. Skrbek *et al.*, J. Low Temp. Phys. **146**, 537 (2007).

[2] M. Blazkova, D. Schmoranzer, and L. Skrbek, Phys. Rev. E **75**, 025302 (2007).

[3] D. Schmoranzer, M. Král'ová, V. Pilcová, W. F. Vinen, and L. Skrbek, Phys. Rev. E **81**, 066316 (2010).

[4] M. Blazkova, D. Schmoranzer, L. Skrbek, and W. F. Vinen, Phys. Rev. B **79**, 054522 (2009).

[5] D. O. Clubb, O. V. L. Buu, R. M. Bowley, R. Nyman, and J. R. Owers-Bradley, J. Low Temp. Phys. **136**, 1 (2004).

[6] M. Blažková, M. Človečko, V. B. Eltsov, E. Gažo, R. de Graaf, J. J. Hosio, M. Krusius, D. Schmoranzer, W. Schoepe, L. Skrbek *et al.*, J. Low Temp. Phys. **150**, 525 (2008).

[7] G. Sheshin, A. A. Zadorozhko, E. Rudavskii, V. Chagovets, L. Skrbek, and M. Blazhkova, Low Temp. Phys. **34**, 875 (2008).

[8] M. Blažková, M. Človečko, E. Gažo, L. Skrbek, and P. Skyba, J. Low Temp. Phys. **148**, 305 (2007).

[9] D. I. Bradley, M. J. Fear, S. N. Fisher, A. M. Guénault, R. P. Haley, C. R. Lawson, P. V. E. McClintock, G. R. Pickett, R. Schanen, V. Tsepelin *et al.*, J. Low Temp. Phys. **156**, 116 (2009).

[10] D. I. Bradley, P. Crookston, S. N. Fisher, A. Ganshin, A. M. Guénault, R. P. Haley, M. J. Jackson, G. R. Pickett, R. Schanen, and V. Tsepelin, J. Low Temp. Phys. **157**, 476 (2009).

[11] D. Schmoranzer and L. Skrbek, J. Phys.: Conf. Ser. **150**, 012048 (2009).

[12] D. Schmoranzer, M. La Mantia, G. Sheshin, I. Gritsenko, A. Zadorozhko, M. Rotter, and L. Skrbek, J. Low Temp. Phys. **163**, 317 (2011).

[13] A. Salmela, J. Tuoriniemi, and T. Rysti, J. Low Temp. Phys. **162**, 678 (2011).

[14] H. A. Nichol, L. Skrbek, P. C. Hendry, and P. V. E. McClintock, Phys. Rev. E **70**, 056307 (2004).

[15] D. Charalambous, L. Skrbek, P. C. Hendry, P. V. E. McClintock, and W. F. Vinen, Phys. Rev. E **74**, 036307 (2006).

[16] V. B. Efimov, D. Garg, M. Giltrow, P. V. E. McClintock, L. Skrbek, and W. F. Vinen, J. Low Temp. Phys. **158**, 462 (2010).

[17]From ECS Inc. International, Olathe, Kansas, USA, [http://www.ecsxtal.com/].

[18] Deepak Garg, Ph.D. thesis, Lancaster University, UK, 2010.

[19]P. C. Hendry and P. V. E. McClintock, Cryogenics **27**, 131 (1987).

[20]P. Skyba, J. Low Temp. Phys. **160**, 219 (2010).

[21]D. I. Bradley, M. Človečko, S. N. Fisher, D. Garg, E. Guise, R. P. Haley, O. Kolosov, G. R. Pickett, V. Tsepelin, D. Schmoranzer, and L. Skrbek , Phys. Rev. B **85**, 014501 (2012).

[22]T. D. Rossing, D. A. Russell, and D. E. Brown, Am. J. Phys. **60**, 620 (1992).

[23]D. D. Awschalom and K. W. Schwarz, Phys. Rev. Lett. **52**, 49 (1984).

[24]A. L. Fetter, Phys. Rev. A **136**, 1488 (1964).

[25]A. V. Gruzinov, Astrophys. J. **498**, 458 (1998).

[26]P. M. Morse and K. U. Ingard, *Theoretical Acoustics* (McGraw-Hill, New York, 1968).

[27]L. D. Landau and E. M. Lifshitz, *Fluid Mechanics* (Butterworth and Heinemann, Oxford, 1987).

[28]H. Yano, Y. Nago, R. Goto, K. Obara, O. Ishikawa, and T. Hata, Phys. Rev. B **81**, 220507 (2010).

[29]D. I. Bradley, S. N. Fisher, A. M. Guénault, R. P. Haley, V. Tsepelin, G. R. Pickett, and K. L. Zaki, J. Low Temp. Phys. **154**, 97 (2009).

[30]H. A. Nichol, L. Skrbek, P. C. Hendry, and P. V. E. McClintock, Phys. Rev. Lett. **92**, 244501 (2004).

[31]W. F. Vinen, L. Skrbek, and H. A. Nichol, J. Low Temp. Phys. **135**, 423 (2004).

[32]D. R. Poole, C. F. Barenghi, Y. A. Sergeev, and W. F. Vinen, Phys. Rev. B **71**, 064514 (2005).